

The local structure of molten polyethylene

Geoffrey R. Mitchell, Richard Lovell and Alan H. Windle

Department of Metallurgy and Materials Science, University of Cambridge, Pembroke Street, Cambridge CB2 3QZ, UK

(Received 9 December 1981)

Wide-angle X-ray scattering provides a direct link to the local structure of non-crystalline materials. Methods of obtaining structural parameters from the scattering functions are described. Comparison of both scattering and real space functions calculated from a wide range of models with those obtained by experiment shows that the chains in molten polyethylene are irregular. The measurements confirm that the chain conformation comprises 60% *trans* bonds and 40% *gauche*, the sequences being random apart from the exclusion of pairs of *gauche* of opposite sign, and that the energy difference between the *trans* and *gauche* states is between 500–700 cal mol⁻¹. The packing of the irregular chains is modelled using a novel approach based on the geometry of randomly packed spheres. There is no evidence for significant correlation of segmental orientation.

Keywords Molten polyethylene; polymer melt; X-ray scattering; randomly packed spheres; molecular conformation; chain packing

INTRODUCTION

Recent small-angle neutron scattering experiments have added significantly to the evidence for an interpenetrating random coil structure for non-crystalline polymers in general, and for molten polyethylene (PE) in particular^{1–3}. However, although there is broad agreement on the nature and characteristic dimensions of chain trajectories, there is still some uncertainty regarding the local structure of the molecular segments. In this context the term 'local structure' is seen as embracing both the spatial and orientational correlations, as well as the local conformation, of the chain segments.

Despite the apparent suitability of X-ray (or electron) diffraction methods for structure analysis in the range 3–30 Å and general agreement over the form of the data, different and even contrasting conclusions seem to have been drawn as to the nature of the local structure. This is particularly true for the melt phase of polyethylene which is, chemically, one of the simplest polymers, and it is salutary to compare, for example, the conclusions of references 4 and 5. This paper presents an approach to the analysis of the X-ray scattering data for molten polyethylene which enables a wide range of possible structural models to be critically assessed. It is a full account of work which was originally outlined at the 1979 Faraday Discussion Meeting⁶.

EXPERIMENTAL

The material used in this investigation was a high density polyethylene, Rigidex 50 (BP Chemicals). The X-ray scattering intensity was measured using a symmetrical reflection diffractometer with MoK α radiation over a range of s from 0.25 to 10 Å⁻¹ ($s = 4\pi \sin \theta / \lambda$). The high viscosity of the melt meant that it was possible to utilize an existing high temperature stage, mounted horizontally. The sample was contained within a copper boat 10 × 15 × 2 mm at 140°C and the sample chamber

evacuated to a pressure of 0.1 torr. The raw intensity data were smoothed and corrected using the procedures outlined elsewhere⁷, the absorption correction taking into account the particular geometry of the sample cell.

It is convenient to display the data as the s -weighted reduced intensity function (or interference function), $i(s)$, given that:

$$i(s) = kI_{\text{corr}}(s) - \sum_{i=1}^n f_i^2(s) \quad (1)$$

where $I_{\text{corr}}(s)$ is the fully corrected intensity, k a scaling factor and $\sum f_i^2(s)$ is the independent scattering from one chemical repeat unit of n atoms.

The $i(s)$ curve obtained in this work is shown in Figure 1, and it is in broad agreement with similar functions already published^{4,8,9}. The corresponding atomic radial distribution function (*RDF*) is obtained by Fourier transformation of the intensity function and is designated $G(r)$:

$$G(r) = 4\pi r(\rho(r) - \rho_0) = \frac{2}{\pi} \int_0^{\infty} sZ(s) \sin rs ds \quad (2)$$

where $Z(s) = i(s)/g^2(s)$ and $g^2(s)$ is a sharpening function usually $|\sum f_i(s)|^2$. Termination error due to the finite range of the data was minimized by using the sampling procedure previously described¹⁰. The inherent resolution of the *RDF* was $\pi/11.0 \text{ \AA}^{-1} \approx 0.3 \text{ \AA}$.

The variety of ways in which an *RDF* may be presented poses problems in comparing functions derived by different authors. For example, different r weightings may be applied to $G(r)$ such as $G(r)/r$ ⁹; $G(r)$ ⁴; and $rG(r)$ ⁵. Equally it is possible to calculate the corresponding electronic functions^{10,11} in which $g^2(s)$ is set to 1. Figure 2 shows two different presentations calculated using the

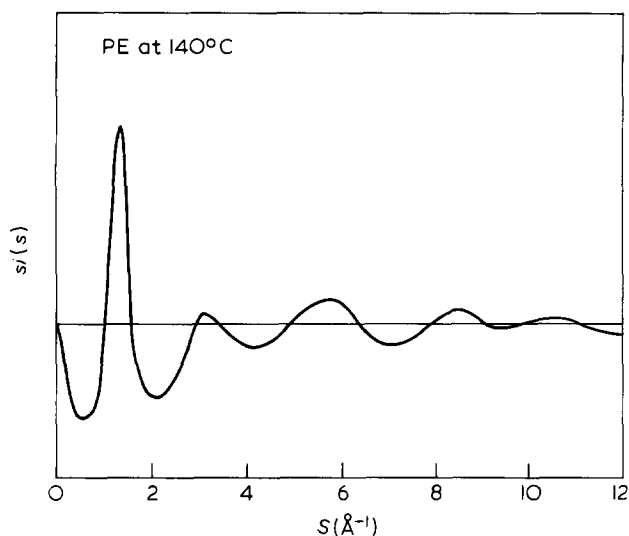


Figure 1 Reduced and s -weighted intensity function $s_i(s)$ of molten polyethylene (PE) at 140°C

intensity data obtained in this work. Curve (a) is $G(r)$ calculated with $g^2(s) = |\sum f_i(s)|^2$, to give the atomic RDF , whereas curve (b) is the electronic function calculated with $g^2(s) = 1$. The two curves are plotted on scales which produce similar maxima. It is clear that although these functions represent the same structure (derived from the same intensity data), they accentuate different features in the RDF , and accordingly care should be taken in their description and comparison, particularly with regard to the damped oscillation beyond 4 \AA . However, when properly corresponding functions are compared the current results are in good agreement with those published^{4,5,9}.

SCATTERING FROM NON-CRYSTALLINE POLYETHYLENE AND LIQUID N-ALKANES

Scattering studies of molten PE and n-alkanes have been a focus of interest since the early X-ray work of Stewart¹² and Katz¹³, who concluded that the samples examined consisted of regions of aligned molecules. Warren¹⁴, on the basis of intensity calculations for a simple model, proposed a structure in which the chains assumed random positions and orientations, although the immediate neighbours about any one molecule were seen as lying roughly parallel. Comparison of electron diffraction patterns of amorphous irradiated and molten PE, with a theoretical analysis of the scattering from straight chains, led Charlesby¹⁵ to the conclusion that the chains are tangled and irregular. However, since then, more quantitative studies have been possible, and these are reviewed below.

Molten PE

Earliest among the more recent studies are the electron diffraction measurements of the Russian workers (Ovchinnikov *et al.*⁵) who analysed their results using RDF 's. Their plots of $rG(r)$ always have an obvious termination ripple. They were well aware of this but ignored it since they were primarily interested in the broad intermolecular peaks at $\sim 5.0 \text{ \AA}$ and beyond. The presence of three such peaks was taken to mean that the chains must lie parallel. By using the position of the first of these peaks and an arbitrary correction for the width of

the 'molecular core', a chain spacing was derived which was (perhaps fortuitously) in very good agreement with the measured density.

Voigt-Martin and Mijlhoff⁴ extended the electron diffraction data to $s \approx 23 \text{ \AA}^{-1}$ but came to completely different conclusions from Ovchinnikov *et al.* They concentrated on the region of the RDF below 8 \AA and took the presence of similar sized peaks at $\sim 3.0 \text{ \AA}$ and at 3.9 \AA to show similar concentrations of *gauche* and *trans* bonds. They also maintained that the broad oscillations in the RDF at 5.0 and beyond are artifacts of the intensity correction procedure related to the finite range of intensity data available. Although they concluded that there are no peaks in the RDF beyond 10 \AA , their RDF ⁴ is basically quite similar to that of Ovchinnikov *et al.*⁵ when it is realised that one is a plot of $G(r)$ and the other is a plot of $rG(r)$. In fact all the RDF 's of Ovchinnikov *et al.*⁵ for PE melts also show peaks or shoulders at $3.0\text{--}3.2 \text{ \AA}$ and at $3.9\text{--}4.0 \text{ \AA}$ although the authors drew no attention to them.

Longman, Wignall and Sheldon⁹ produced RDF 's from X-ray diffraction data up to $s = 16 \text{ \AA}^{-1}$ and, despite the termination ripple, the peaks are apparently in very similar positions to those of both Voigt-Martin and Mijlhoff and Ovchinnikov *et al.* They concluded that the chains have random conformations with intermolecular peaks which represent liquid-like order.

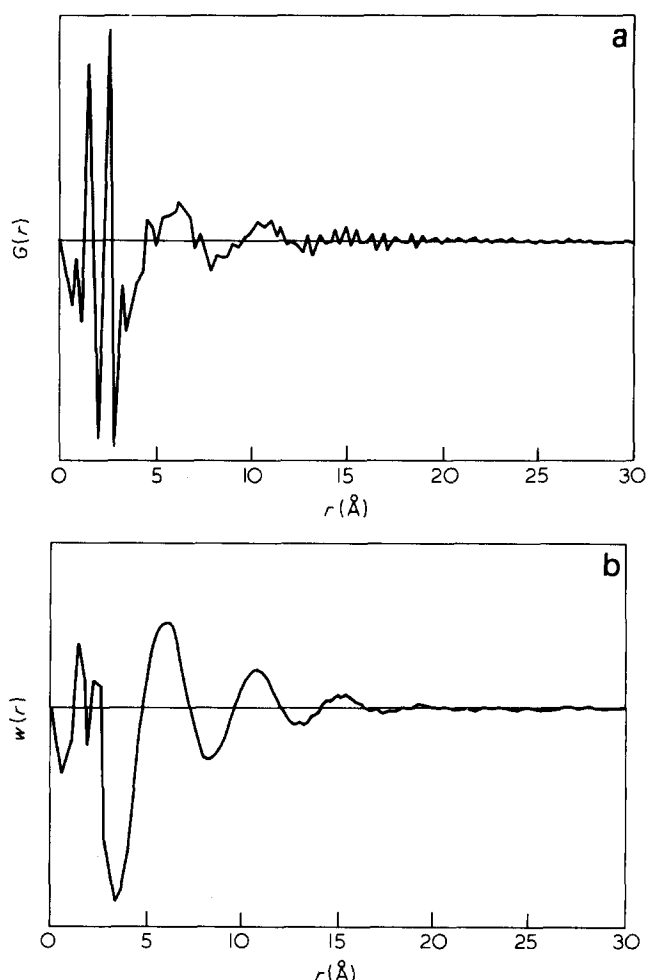


Figure 2 Radial Distribution Functions (RDF 's) of molten PE at 140°C each prepared from the same experimental data. Plot (a) is an atomic RDF ($G(r)$), whereas (b) is the unsharpened electronic equivalent ($W(r)$)

Kan and Seto¹⁶ have also made X-ray measurements and derived an *RDF* similar to the others, although with rather less termination ripple. Despite the presence of a small peak at 3 Å, they concluded that much of the material exists in bundles of chains in an extended conformation of about 10 carbon atoms. They calculated the intensity expected from a hexagonal paracrystalline model and this is in good agreement with the measured intensity. Unfortunately the average chain spacing in the model is 5.5 Å which gives a density much lower than is observed.

Pechhold, Hauber and Liska¹⁷ used a diffraction pattern generated from an optical mask to provide qualitative arguments for the acceptance of the meander model for PE melt. (This model is discussed in detail in the 'Testing Established Models' section later.) Whereas a form of bundle model was proposed by Petermann and Gleiter¹⁸ on the basis of observations using electron microscopy and diffraction on thin films of molten PE at 190°C.

Fischer *et al.*^{8,19} have argued that the *RDF*'s of molten PE and liquid n-alkanes are insensitive to correlation of chain orientation. They attribute the broad peaks at 5, 10, 15 Å in the *RDF* to interchain packing arising from short-range order expected for geometrical reasons, although they have presented no quantitative model to support this view.

Amorphized PE

Solid PE amorphized by radiation has been studied by Ovchinnikov *et al.*⁵, Yoda *et al.*²⁰ and by Gupta and Yeh²¹. The *RDF*'s presented by these investigators do not show any hint of a peak at 3.0 Å (the peak related to the presence of *gauche* bonds). In most other respects, however, Ovchinnikov's *RDF* is very similar to those from PE melts. In contrast Yoda's *RDF* shows a much more slowly damped intermolecular oscillation. This is not surprising since the first peak in the scattering pattern is much sharper than for molten PE and is also at a higher *s* value. Gupta and Yeh analysed their *RDF* of amorphized PE using the paracrystalline lattice theory. The amorphous component of a semicrystalline sample of PE has also been subjected to an analysis based upon the paracrystalline approach²¹.

From these results it seems that amorphized PE probably has considerably more order than molten PE. This is particularly true when the amorphized material is oriented as well⁵, whereupon the cylindrical distribution function shows a high degree of order parallel to the extension axis, corresponding to fully extended chain segments at least 15 Å long.

Liquid n-alkanes

Recently n-alkanes have received some attention because of the observation of weak orientational correlations using the techniques such as depolarized light scattering and magnetic birefringence. These measurements and their implications have been reviewed by Boyer²² and by Fischer and Dettenmaier⁸.

Ovchinnikov *et al.*²³ have examined the effect of temperature on the positions and widths of peaks in the scattered intensity for a series of alkanes from C₉ to C₂₄. They observed an odd-even effect when the first peak position is plotted as a function of $(T - T_m)$ which, since the scattering was analysed in terms of parallel chains, was

used to support the bundle type model. However the effect might be more usefully attributed to the odd-even effect in the melting temperature. Kan and Seto⁶ compared the *RDF*'s for molten C₃₄ with the *RDF* for a solid crystalline sample of C₂₈ and also the *RDF* for molten PE. The *RDF*'s of the two melts are very similar, with shoulders at 4 Å and ~3 Å, whereas the *RDF* for the crystalline sample only exhibits a shoulder at 4 Å. Similar effects were observed by Longman, Wignall and Sheldon⁹, in their observations of a range of alkanes. They attempted to use the number of broad oscillations in the *RDF* as a measure of order although, considering the termination ripple present, a better measure would be the width of the main peak in $i(s)$ ²⁴. Longman *et al.*⁹ conclude that the maximum order is observed for alkanes of $n = 16$ and that the positions of the broad maxima are consistent with hexagonal chain packing.

A different type of analysis was presented by Brady and Fein²⁵. They examined the low angle side of the principal peak in the scattering function for a range of alkanes and found a small shoulder which had been previously discussed by Stewart *et al.*¹² in connection with long chain alcohols and acids. They suggested that the position of this peak in the scattering may be related to the overall length of the molecules, and that its variation within the alkane series suggests the presence of extended chains.

WIDE ANGLE X-RAY SCATTERING (WAXS) ANALYSIS

The position of peaks, either in the *RDF* or in the scattering function $si(s)$, does not give immediately useful information on the molecular organization in the polymer sample, the only readily assignable features in the *RDF* being the peaks at 1.5 Å and 2.5 Å which represent the distances within the chain which are fixed by covalent bonding. However, careful analysis of the scattering, or of the *RDF* beyond 2.5 Å, can give detailed information about the conformational, spatial and orientational order. This analysis is made by comparing the experimental scattering pattern or *RDF* with similar functions calculated from a wide range of possible three-dimensional models^{6,7}.

Any such analysis will be facilitated if the *RDF* or $si(s)$ function can be partitioned into features arising from correlations within chains (intra-chain), and those arising from between chains (inter-chain). For glassy polymers we have identified the inter- and intra-chain features by examining the scattering from oriented material^{26,27}, and by calculating cylindrical distribution functions²⁸. The corresponding technique for the case of molten PE would require special ingenuity, although some indications may be drawn from observation of changes in peak position temperature as exploited in previous work on polystyrene²⁹, or by analogy with similar polymers which are available as glasses.

Ovchinnikov *et al.*⁵ have calculated the projections of the Cylindrical Distribution Function (*CDF*) for solid oriented amorphized PE. The equatorial (normal to the extension axis) projection contains the prominent broad peaks at 5, 10 and 15 Å which are observed in the *RDF*'s for molten PE. Whereas for the projection parallel to the extension axis, these peaks are considerably diminished. This suggests an inter-chain origin for the broad peaks in the *RDF*, and for their corollary in the scattering function

which is the major peak at 1.3 \AA^{-1} . The broad similarity of the *RDF*'s of molten PE and amorphized PE tempts one to draw the same conclusions for molten PE, that is, the inter-chain nature of the intense peak at 1.3 \AA . This inter-chain nature has been tacitly assumed by the majority of workers, usually on the basis of simple geometric reasoning.

In this paper we make the initial assumption that features in the scattering representing inter-chain correlations are confined to s values $< 2.0 \text{ \AA}^{-1}$, and justify it later in the 'Spatial and Orientation Distributions' section. Such an approach enables the scattering at s values $> 2.0 \text{ \AA}^{-1}$ to be compared with that calculated from models of single chains. The analysis is carried out first with comparisons of scattering rather than the *RDF*(s). Principally, this is because the form of the $si(s)$ function is much more sensitive to the regularity in the chain than is the *RDF*. In the *RDF*, significant peaks due to long regular sequences along the molecule would occur at $r > 5 \text{ \AA}$, where they would be confused with the main contribution from inter-chain distances.

Atomic coordinates for the various models are calculated using a chain building computer routine. The bond lengths C–C and C–H are fixed at 1.54 \AA and 1.1 \AA respectively and the valence angles, CCC at 112° and HCH at 110° . Interatomic distances are calculated from these coordinates and $si(s)$ thus generated from the Debye scattering equation³⁰:

$$Ni(s) = \sum_{j \neq k}^N \sum_{k}^N f_j(s) f_k(s) \sin r_{jk}s / r_{jk}s \quad (3)$$

where N is the number of atoms in the model, r_{jk} is the distance between the j th and k th atoms and $f_j(s)$ the atomic scattering factor for the j th atoms³¹. (For the hydrogen atoms we have used the scattering factor for neutral hydrogen which must be considered an approximation.) Owing to the limited extent of the models, there is always a strong peak in the calculated $si(s)$ near to the origin and extending to $s \approx 1 \text{ \AA}^{-1}$. (It would be centred at the origin if the function plotted was $i(s)$.) This peak is effectively the scattering from a uniform distribution of electron density with the same shape as the model. For modelling with single chains, where we are only concerned with the region beyond $s = 2.0 \text{ \AA}^{-1}$, this peak is of little consequence, but it must of course be removed before data-model comparisons can be made over the complete range of s . This can be done by effectively embedding the model in a continuum with electron density equal to the average for the model. A spherical model is most easily handled by this technique, although a procedure for more general shapes has been proposed³². The correction is made by subtracting the scattering from a sphere of the same size as the model but with uniform electron density. This scattering is given by Guinier and Fournet³³.

$$I(s) = \left| \sum_i^n f_i(s) \right|^2 9(\sin Rs - Rs \cos Rs)^2 / (Rs)^6 \quad (4)$$

where R is the radius of the sphere.

The model *RDF*'s are calculated using procedures which first introduce the smearing components due to finite data limits and thermal vibrations, and then subtract the average density to give a reduced *RDF*^{7,32}.

LOCAL CONFORMATION

In general the bond lengths and valence angles of a polymer molecule are almost independent of whether it is in the crystalline or non-crystalline state, the difference in conformation being due to the much less regular sequences of backbone rotation angles for the non-crystalline case. Hence the problem of determining the local structure reduces to establishing a specification of the distribution of rotation angles. The number of numerically possible conformations may be drastically reduced, if the conformations which would result in severe atom-atom overlap are discarded. The procedures by which the more probable conformations may be identified are discussed first, and then the scattering calculated for chains in those conformations compared with the experimental scattering functions.

Conformational analysis

Although considerable information may be gleaned from examination of space-filling molecular models, the most convenient method for systematically evaluating probable conformations, is by means of empirical conformational energy calculations. This type of analysis has been used extensively in the derivation of molecular trajectories for a wide range of polymers, including several analyses for representative sections of PE chain³⁴⁻³⁸. Usually the total energies calculated for different conformations are plotted as contours on a map with the backbone rotation angles (ϕ_1, ϕ_2) as coordinates. The section of chain used in the calculations is usually small (~ 5 skeletal atoms), and the variations in the rotation angles are restricted to the two central bonds. The alternative approach is to vary all of the chain parameters in such a manner that the total conformational energy is minimized (for example, see ref 39). This technique although having less constraints does not, as a map does, indicate the broad areas of conformation which are possible or prohibited. For the important but somewhat limited role which energy calculations play in this analysis, we have found the maps considerably more useful. It is not our intention to dwell on the precise methods used in such calculations, since they have been adequately described elsewhere (e.g. ref 40), but rather to consider the application of such procedures in the context of this analysis, which is essentially based on X-ray scattering.

In the case of a representative section of PE chain in which the partial charges or dipoles are minimal⁴¹, summation of the contributions to the conformational energy may be restricted to the terms relating to the non-bonded atom interactions and the intrinsic torsional potentials for the skeletal bonds. It is conventional to restrict the non-bonded potentials to pair-wise interactions using a 6-12 Lennard-Jones function:

$$U(r) = \frac{B}{r^{12}} - \frac{A}{r^6} \quad (5)$$

The coefficients (A) of the attractive component may be calculated using the Slater-Kirkwood formulation (p 45 of ref 40). The coefficients (B) of the repulsive component are then adjusted to give a minimum for $U(r)$ at an r value corresponding to those observed in known structures, usually crystalline⁴¹. The intrinsic torsional potential is

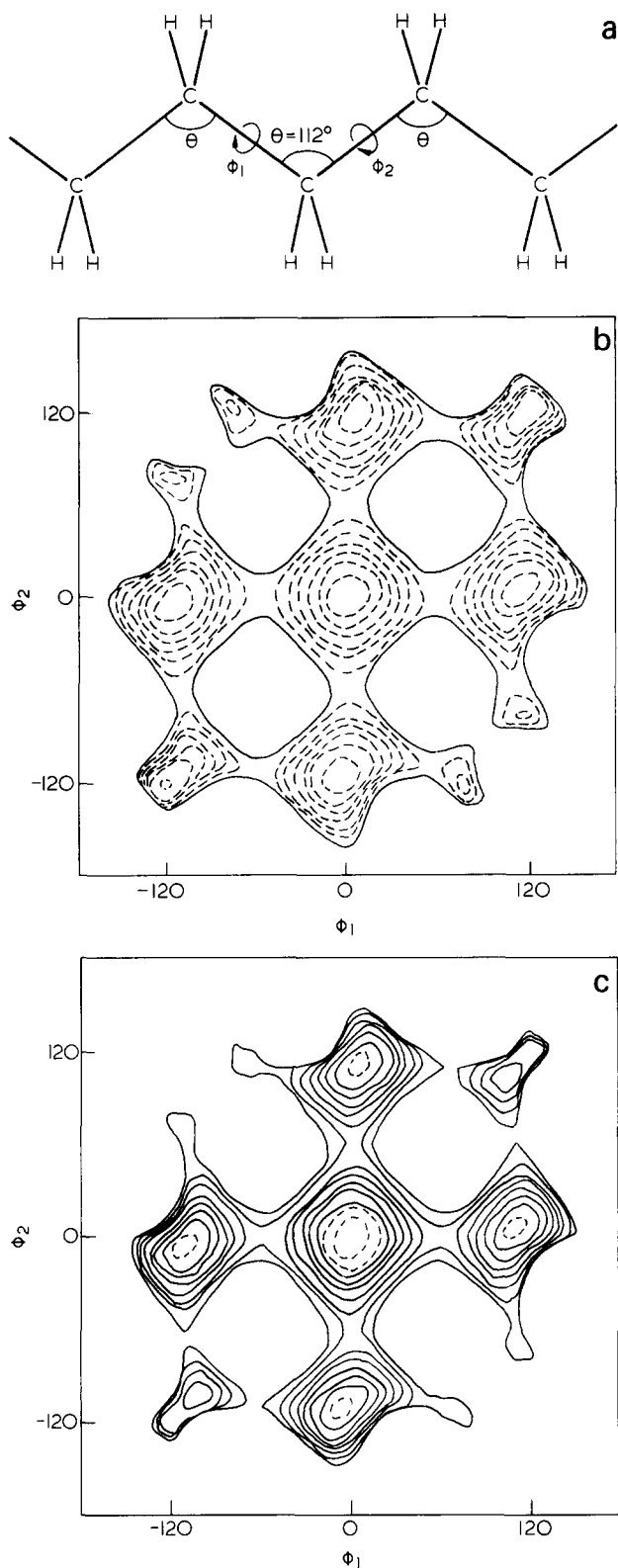


Figure 3 (a) Sketch of a segment of the PE molecule on which the angles relevant to the energy calculations are marked. Parameters are listed in *Table 1*. (b) Conformational energy map for a segment of a polyethylene molecule. (c) Equivalent energy map to (b) showing the relatively small effect of increasing atomic size by 10%. Broken contours negative. Contour interval 0.5 Kcal

obtained from spectroscopic studies of small molecules. As a consequence, the values assigned to the energy parameters are effectively defined by the size adopted for the component atoms. The size or contact radii have similar values to the Van der Waals radii. Recently Atkins, Isaac and Keller⁴² have shown, for isotactic polystyrene,

that small changes in the values for these radii may produce large changes in the energy map. One common practice is to add 0.1 Å to the radii observed in crystalline structures (Brant, Miller and Flory⁴³). In order to ascertain the sensitivity of previous calculations to the parameters chosen, we have repeated the energy calculations for differing atom sizes. The geometry of the chain section for which the calculations were performed is shown in *Figure 3a* and the values of the constants used are detailed in *Table 1*. Employing the normal intrinsic torsional potential (for example, see ref 44) and coefficients for the 6-12 potential from Momany *et al.*⁴¹, the conformational energy map shown in *Figure 3b* is obtained. This is in excellent agreement with previous calculations. *Figure 3c* shows an equivalent energy map drawn for atoms 10% larger than the accepted values. Decreasing the atomic size by a corresponding amount has a similarly small effect. It is obvious that for PE type sections the form of the energy map is relatively insensitive to the precise values assigned to the atomic parameters. This in part is due to the lack of any drastic steric hindrance at rotations less than 100° which means that the maps are dominated by the intrinsic torsional potential.

These calculations have been performed on a small section of a PE chain (5 backbone atoms) in which only the central bond rotation angles have been varied, although for regular conformations such as helices, it may be appropriate to consider a more constrained regular model.

The next step is to use the information obtainable from these energy maps as a guide in the preparation of models for scattering comparisons.

Intra-chain scattering

Despite the limitation of the range of backbone rotation angles made possible by steric considerations, there remains a multitude of conformations to be examined. As a starting point and in order to make the general survey of possible conformations tractable, we will adopt the axioms of the rotational isomeric state theory (Volkenstein⁴⁵). In the context of this simplification, inspection of the energy map (*Figure 3b*) shows that there are seven broad minima, at combinations of 0°, 120° and -120°, which can be assigned to the rotation states *tt*, *tg*, *gt*, *t \bar{g}* , *g \bar{t}* , *gg* and *g \bar{g}* . The first comparisons between the scattering calculated for models using equation (3) and the experimental *si(s)* will be made for chains consisting of simple regular arrangements of these rotation states.

Regular conformations. In addition to the type of conformation, the length over which it persists is an equally important structural parameter. To examine this variable, initial comparisons will be made for chains

Table 1 Constant values used in energy calculations

Atom	r_0	Atomic polarizability (α) $\alpha \times 10^{24} \text{ cm}^3$	Effective number of outer shell electrons N_{eff}
H	1.2	0.42	0.85
C	1.70	0.93	5.20

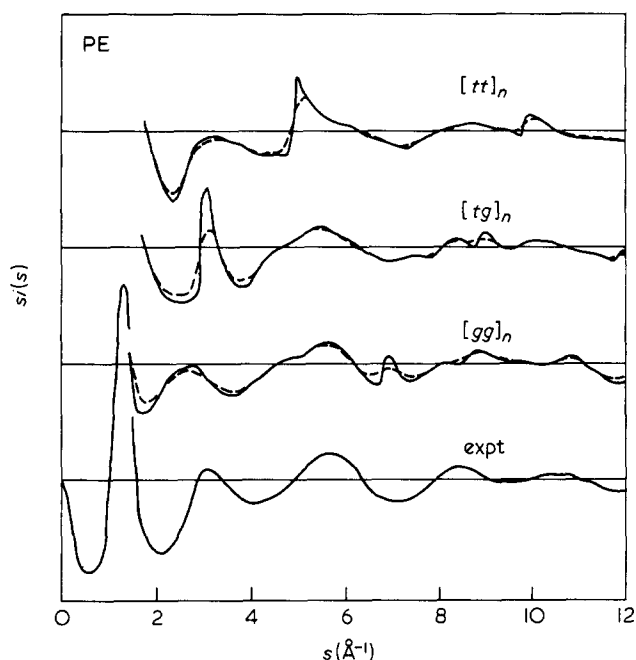


Figure 4 Calculated $si(s)$ curves of PE molecules in the conformations $(tt)_n$, $(tg)_n$ and $(gg)_n$ for run lengths of 12 (---) and 48 (—) backbone bonds. The calculated functions are compared with the experimental function

consisting of 12 and 48 skeletal bonds. The $si(s)$ curves calculated for chains in $(tt)_n$, $(tg)_n$ and $(gg)_n$ conformations are shown in Figure 4. The conformations $(g\bar{g})_n$ and $(\bar{g}g)_n$ are not considered as they involve considerable atom-atom overlap. The agreement between the calculated and the experimental curves is poor for any of the conformations, although some similarity may be seen in the short sequences particularly for the all-*trans* chain. In general the presence of all-*trans* sequences leads to peaks in the calculated scattering function at approximately the observed locations, although they are too sharp.

On the basis of the curves shown in Figure 4 it is concluded that the PE melt structure does not contain any significant proportion of long sequences in regular conformations. However, the comparisons have been made for perfectly regular conformations without any compensation for thermally induced torsional variations. An appreciation of the magnitude of this type of effect may be obtained from the conformational energy analysis. The simplest approximation appropriate to the map of polyethylene is a Gaussian distribution of skeletal bond rotations with a standard deviation of 10° . In order to obtain a reasonable statistical sample of this distribution, the average of a number of chains is required. This problem may be overcome by considering a long chain (500–1000 bonds), which removes any end effects. However such a chain may turn back on itself and generate near-neighbour distances which are effectively inter-chain in nature. These distances may be excluded by calculating the scattering for only those atom pairs which are separated by less than n skeletal bonds along the chain. The restriction, when properly judged, has no other effect on the result, but greatly reduces computational time. This approach is used for all subsequent calculation of scattering from random chains. The scattering thus calculated for the same regular conformations as in Figure 4, but with randomly distributed variations in torsional angles, is shown in Figure 5. Although there are slight improvements, the overall agreement is still poor.

Irregular conformations. Since no regular conformation provides a satisfactory match to the data, the next step is to take the most promising conformational sequence and introduce defects in the form of other conformations. This is most easily achieved by 'building' a chain according to a set of unconditional probabilities. The probability of the next rotation state being *trans* is p_t while the probability of it being *gauche* + is $(1-p_t)/2$. Figure 6 shows the $si(s)$

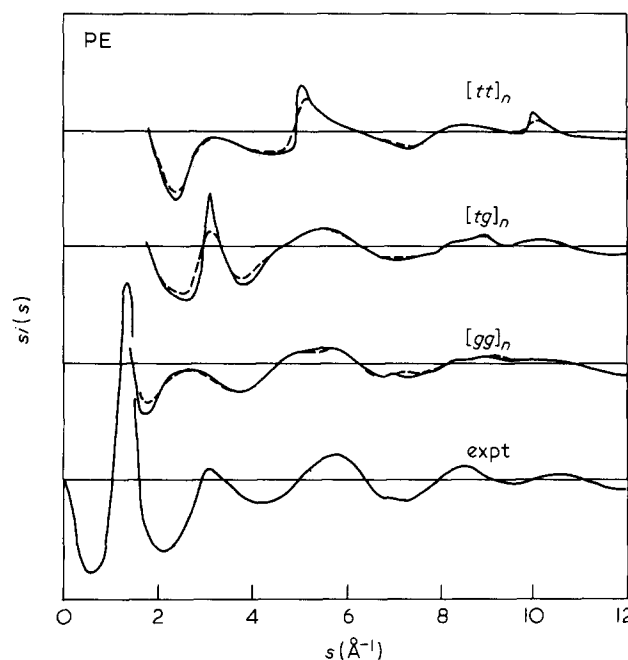


Figure 5 An equivalent diagram to Figure 4, with the exception that the torsional angles (ϕ 's) have Gaussian distributions about the mean values with a standard deviation of 10°

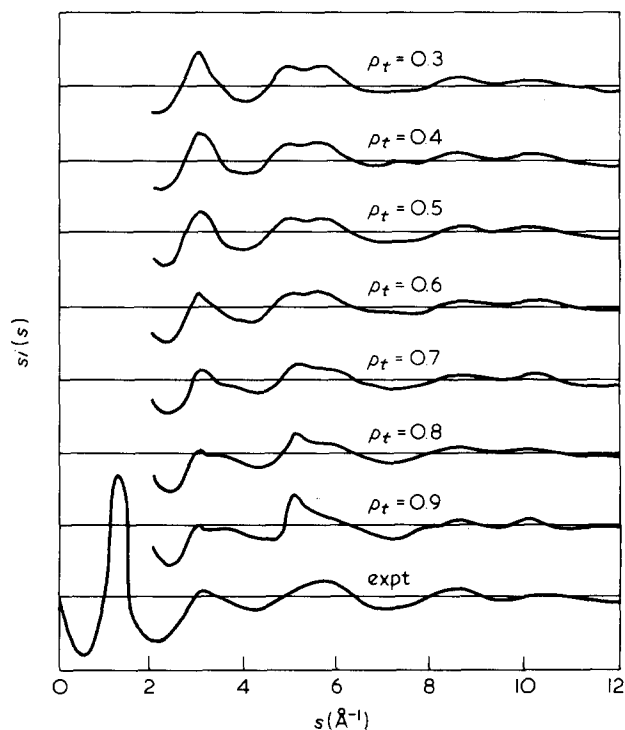


Figure 6 Calculated $si(s)$ curves for chains with three rotational isomers (*t*, *g* and \bar{g}) distributed at random using unconditional probabilities showing the effect of assigning P_t a range of values. Comparison is again made with the experimental curve

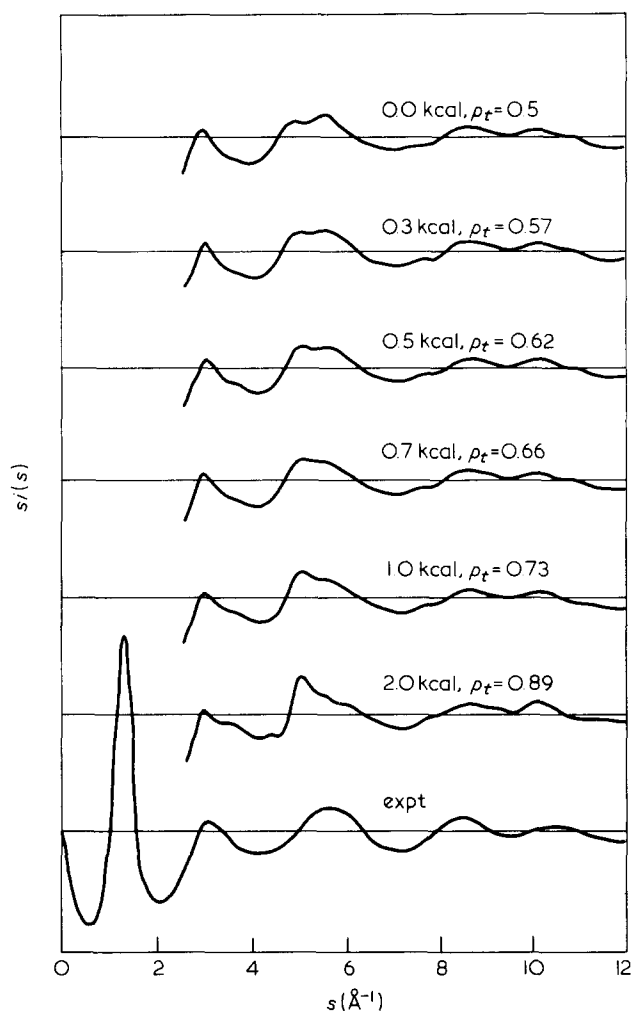


Figure 7 Calculated $s(i)s$ curves prepared using conditional probabilities, plotted for a range of P_t values corresponding to the energy differences between *trans* and *gauche* as shown

curves calculated for random chains consisting of 500 skeletal bonds (although the correlation for scattering purposes was restricted to ~ 20 bonds), built using different values of p_t . Reasonable agreement between experimental and calculated $si(s)$ curves is obtained in the range $p_t = 0.5$ to 0.7 . There remains some discrepancy between the scattering calculated for the models and the experimental scattering, particularly in the finer detail of the peak centred at 5.0 \AA^{-1} . In order to improve the model, it is instructive to re-examine the energy analysis.

The analysis of the local conformation of PE melt has so far only utilized the energy calculations to select probable conformations, no attempt has been made to use the energy values to evaluate or predict the proportions or the distribution of rotation states. Statistical mechanical procedures which employ such information have been extensively used for deriving molecular trajectories⁴⁶. The relative energy levels of the minima (strictly the areas about each minimum) are incorporated into the analysis through statistical weight matrices. Each element of the matrix u_{ij} is related to the energy penalty for rotation state j , rather than state 1 (or *trans*), following state i . If the usual assumptions are made, then the weights may be obtained from the energies by application of Boltzmann statistics. The matrix U for a symmetric chain with three states is given by Flory⁴⁶:

$$U = \begin{bmatrix} 1 & \sigma & \sigma \\ 1 & \sigma\psi & \sigma\omega \\ 1 & \sigma\omega & \sigma\psi \end{bmatrix} \quad (6)$$

where σ is the weighting for a *gauche* (\pm) state following a *trans*, $\sigma\psi$ is the weighting for a pair of *gauche* states of the same sign and $\sigma\omega$ is the weighting for *gauche* bonds of opposite signs. Although this type of matrix may be used directly in the statistical mechanical analysis, for chain model building conditional probabilities are required. These may be obtained for a symmetric homopolymeric chain by a straightforward procedure, (p 91 of ref 46). The conditional probability matrix Q using the weights given by Abe *et al.*³⁵ for PE at 400 K is:

$$Q = \begin{bmatrix} 0.54 & 0.23 & 0.23 \\ 0.683 & 0.291 & 0.026 \\ 0.683 & 0.026 & 0.291 \end{bmatrix} \quad (7)$$

There are two significant aspects of this matrix. The first is that the probability of *trans* following *trans* is about 0.6, a similar value to that obtained from our simple X-ray scattering analysis. The second is that the probability of *gauche* pairs of opposite sign is so low that they are effectively prohibited. In an effort to find the model most compatible with the experimental X-ray evidence we have considered chain conformations where successive rotation states have been assigned according to the above scheme. In order to assess the sensitivity of the scattering calculations to the energy levels, we have varied the value of σ in the matrix (6), working in terms of the energy difference between the *trans* and *gauche* states to which it is directly related, while the values of the remaining weightings are unchanged. Figure 7 shows the $si(s)$ curves for chains 'built' with $E_{gauche} - E_{trans}$ varying from 0–2 kcal mol⁻¹. The best agreement is seen for the value of E_{g-t} of 500–700 cal mol⁻¹, although since the variation in actual probabilities covers a smaller range than in Figure 6, the conclusions appear less firm. This energy difference, as well as being in line with the conformational energy analysis is also in good agreement with the experimental values obtained by spectroscopic methods⁴⁷.

There are a variety of minor refinements which may improve the agreement between the $si(s)$ curve calculated for the model and the experimental one, although the stage has been reached in which refinement is of diminishing consequence to the understanding of the local structure. However, one additional improvement can be made. Initially we adopted rotational isomers to simplify the analysis, although the energy analysis suggests that the values of the rotation angles depend upon the adjacent bonds. These adjustments have been incorporated into a chain with states distributed using the probabilities of the type given in equation (7) with an $E_{gauche-trans}$ of 500 cal mol⁻¹. The scattering curve calculated for this model is shown in Figure 8 together with the experimental $si(s)$. For all values of $s > 2.0 \text{ \AA}^{-1}$ there is close correspondence between the two curves.

The local conformation derived from this X-ray scattering analysis is thus an irregular distribution of *trans* and *gauche* states, with about 60% of the former. The sequences of all-*trans* units in such a chain will have an average run length of 3–4 bonds.

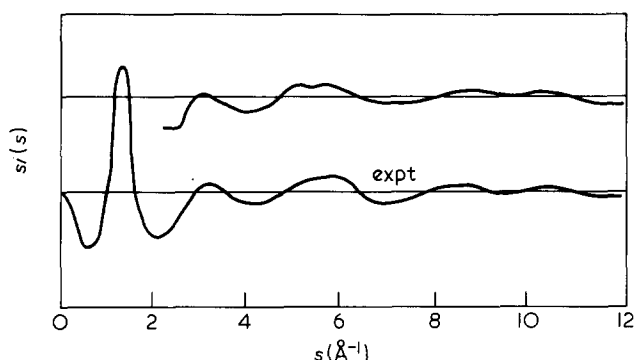


Figure 8 Further refinement of the calculated $s(i)s$ curve of Figure 7 for $E_{gauche} - E_{trans} = 0.5 \text{ Kcal mol}^{-1}$ in which bond rotation angles are adjusted to minimum energy positions

SPATIAL AND ORIENTATIONAL DISTRIBUTIONS

In this section we shall first examine the packing modes which are possible for chains with the local conformation derived in the previous section; secondly the extent of the inter-chain scattering will be evaluated; and finally the effect of orientational correlations will be considered.

Packing analysis

An essential feature of any structural model is its density. Since the density is dependent on the constituent atoms as well as the packing efficiency, we have chosen to use the packing fraction as a parameter in our models. This is the ratio between the volume occupied by the atoms (calculated from their radii) and the total Van der Waal volume. The volume of a CH_2 group was taken from the tabulated values of Slonimskii⁴⁸, while the data used for specific volume of PE as a function of temperature were those of Stewart and Von Frankenberg⁴⁹. At the melting point (410 K) the bulk density of the melt is 783 K g m^{-3} which gives a packing fraction of 0.575. This may be compared directly with the maximum possible for randomly close packed spheres (0.63), close packed spheres (0.74) and hexagonally packed cylinders (0.91).

We have shown previously²⁴ that the intense peak at around $s = 1.3 \text{ \AA}^{-1}$ is inter-chain in origin, and that it does not necessarily relate to parallel chains, reflecting, rather, the consistency of packing arrangements in the material. The principal conclusion of the preceding section is that the typical PE chain is irregular in trajectory with an average all-*trans* sequence of 3–4 bonds followed by a *gauche* state and occasionally by a *gauche-gauche* sequence. The length of these segments or sequences will be about 4–6 \AA . The diameter of a cylinder which encloses a *trans* sequence is 5.1 \AA , and hence the aspect ratio (length/breadth) of an average sequence is about 1. The globular nature of the structural units suggests that it may be reasonable to represent the inter-chain interactions (i.e. between these globular segments) in terms of relations appropriate to randomly packed spheres. A wide variety of algorithms have been developed for constructing three-dimensional models of randomly packed spheres (for example Finney⁵⁰), and using such a model we have inserted into each sphere a typical PE segment. From this three-dimensional model the intensity functions have been calculated using the Debye equation as described above. This model is essentially that for a low-molecular weight alkane, but despite its limited connectivity it

appears to provide a useful and manageable approach to the determination of the influence of orientational correlations on the scattering.

If we consider an assemblage of randomly oriented units without any orientational correlation then the scattering is given by:

$$i(s) = I_m(s)F(s) - \sum_i f_i^2(s) \quad (8)$$

where $I_m(s)$ is the unreduced scattering function for one isolated unit and $F(s)$ is the structure factor for the disposition of the centres of these units. Variants of $I_m(s)$ have been calculated above (e.g. Figure 8) and $F(s)$ could be obtained from a three dimensional model or by the use of an analytical expression. We have used the structure factor for a mono-disperse system of spheres described by the Percus-Yevick theory (Thiele⁵¹), which has been given by Wright⁵² and depends only on the packing fraction (η) and the sphere radius (R).

$$F(s) = 1/(1 - H(s)) \quad (9)$$

where,

$$H(s) = \{ [C_1 - 2C_2/Rs] \\ + [-C_3Rs + C_4/(Rs) - C_2/(Rs)^3] \cos 2Rs \\ + C_5/(Rs) + C_2/(Rs)^3 \} C_0/(Rs)^3$$

and,

$$C_0 = -3\eta/(1-\eta)^4; \quad C_1 = 1 - 6\eta + 5\eta^3; \\ C_2 = (3\eta/2)(1+2\eta)^2; \quad C_3 = 2 - 3\eta + \eta^3; \\ C_4 = (3\eta/2)(-2 + 4\eta + 7\eta^2); \quad C_5 = (3\eta/2)(2 + \eta)^2.$$

Of course a single rigid interaction between segments would be unrealistic, and a distribution of intersegmental distances is required. Solutions for a polydisperse system of spheres has been given recently by Blum and Stell⁵³ and Vrij⁵⁴ but both require extensive computation. Instead, as an approximation to a distribution of sizes, we have adopted an averaged $F(s)$:

$$F(s) = \sum_r w(r)F_r(s) \quad (10)$$

where $F_r(s)$ is the structure factor for spheres of radius r and $w(r)$ is the weighting. This is strictly only applicable to a multiphase system but appears a sensible first approach. The distribution of sphere size was chosen so that the calculated scattering matched both the width and position of the first experimental peak ($s = 1.3 \text{ \AA}^{-1}$). The appropriate distribution was centred at 5.5 \AA which is entirely reasonable on the basis of the known molecular dimensions. The result of modulating the segmental scattering of Figure 8 with the interference function for randomly packed spheres with a packing fraction of 0.575 (equation (8)) is shown in Figure 9. The magnitude of the calculated first peak is in excellent agreement with that of the experimental scattering; moreover the calculated scattering curve at higher scattering vectors is apparently unchanged by the interchain correlations. The absence of inter-chain features in the scattering above $s = 2.0 \text{ \AA}^{-1}$ is

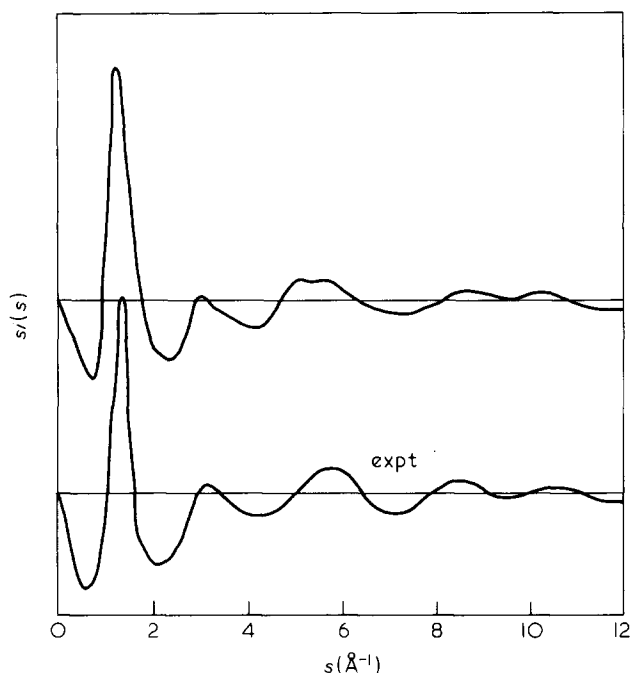


Figure 9 $s_i(s)$ function of Figure 7 (with $E_{gauche} - E_{trans} = 0.5$ Kcal) modulated by an interference function representing the scattering from randomly packed spheres. There is good agreement with the experimental curve over the complete range of s

typical of many non-crystalline polymers (PMMA, PS, etc.), and it enables experimental and model conformations to be compared over a fair range of s without the necessity of modelling the inter-chain effects. Figure 10 (a-d) illustrates that it is the range of sizes of the randomly packed spheres, introduced to model the fact that the polyethylene chain segments are of a much less regular shape than spheres, which accounts for the absence of inter-chain features at larger values of s . Figure 10a is the scattering calculated for randomly packed spheres of uniform size (from equations (8), (9) and (10)), and shows the sharpness of the first peak and the additional features at above $s = 2.0 \text{ \AA}^{-1}$. Figures 10b to 10e show the effect of broadening the size range of the randomly packed spheres. (Figure 10d) is equivalent to the scattering of Figure 9. It thus appears that the sharpness (or otherwise) of the main inter-chain peak in the scattering from non-crystalline polymers is associated essentially with the regularity in the shape of the chain segments and thus the range of nearest-neighbour vector lengths. Since the width of the distribution chosen is reasonable if the appropriate distances are measured on space-filling molecular models, we conclude that a 'random' chain structure, in which there is effectively zero correlation of segmental orientation, satisfactorily reproduces the observed scattering. This does not of course prove that such a structure is topologically possible, neither does it rule out the possibility of a limited degree of orientational correlation. However, recently Ryckaert and Bellemans⁵⁵, and Vacatello *et al.*⁵⁶ and Weber and Helfand⁵⁷ have successfully carried out theoretical packing analyses for alkanes using both molecular dynamical and Monte Carlo methods which have predicted the experimentally observed densities with appropriate conformations. Although these calculations⁵⁵⁻⁵⁷ were carried out using short chains (C_nH_{2n+2} $n = 4, 6, 20$), there seems to be no reason to

doubt that similar models could be generated for long polymer chains, although the computation time required could be prohibitive. The packing analysis we have presented allows a range of models to be examined easily, but it does depend upon the prior determination of a realistic conformation.

Inter-chain scattering

At this stage it is appropriate to justify the original assumption that the scattering function for $s > 2.0 \text{ \AA}^{-1}$ is unaffected by the inter-chain interaction. It has been established that the permanent peak in the $s_i(s)$ function at $\sim 1.3 \text{ \AA}^{-1}$ is inter-chain in origin. The broadness of this peak indicates that there is a range of inter-chain distances, arising from irregularities in shape and packing, although the chain correlation extends beyond the nearest neighbours. A single inter-chain distance will not only give a narrow peak at $s \approx 1.3 \text{ \AA}^{-1}$, but also subsidiary maxima at great s values. This is illustrated in Figure 10a, which was calculated using the packing of random spheres method (equations (5), (6), (7)). The higher orders are damped out to an extent by the inter-chain scattering; this molecular scattering decreasing more rapidly than atomic scattering. When a distribution of sphere sizes is

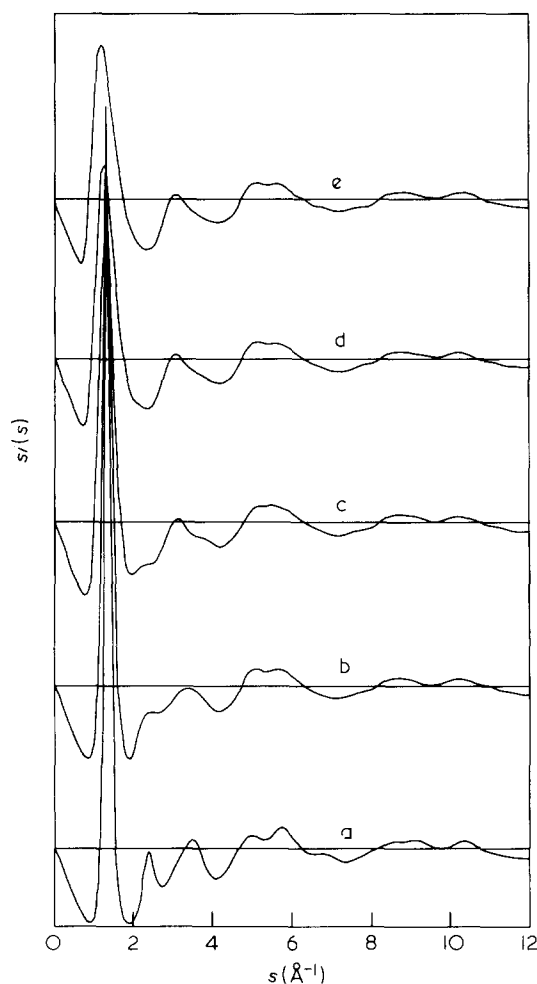


Figure 10 $s_i(s)$ functions illustrating the effect of variations in the size range of the randomly packed spheres. For a range of sizes sufficiently broad to model the width of the first experimental peak, the curve is free from second order intermolecular features. (a) Single sphere size (b-e) sphere sizes with gaussian distribution with standard deviation: (b) 0.25Å, (c) 0.50Å, (d) 0.75Å, (e) 1.0Å

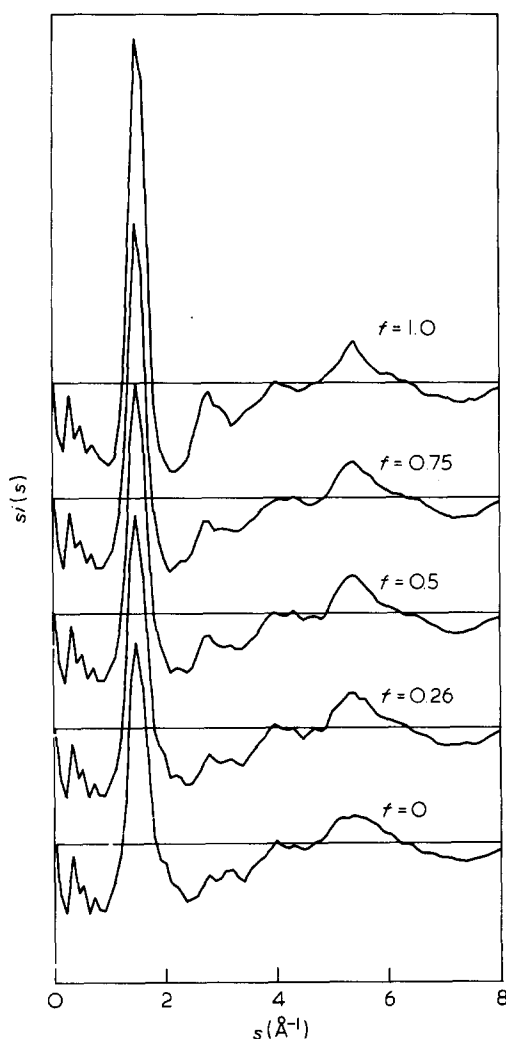


Figure 11 Illustration of the effect of mutual alignment of neighbouring segments of the PE molecule, disposed at the centres of randomly packed spheres on the calculated $s_i(s)$ plot

introduced (Figure 10 b, c, d) not only does the first peak become broader, but in addition the higher order peaks decrease in magnitude. This effect is due to the overlapping of the peaks, and is not a damping effect. We conclude that in order to generate a first order inter-chain peak with the observed width, the level of inter-chain disorder required is such that higher order inter-chain peaks are lost (Figure 10d). Hence in effect, features associated with inter-chain scattering are restricted to s values less than 2.0 \AA^{-1} .

Oriental correlations

In order to model successfully the scattering from PE melt it is not necessary to invoke any orientational correlation of the chains or segments (see 'Packing analysis' section above). In this section we evaluate the effect of mutual alignment of the chain segments on the scattering function. We will consider the possibility of parallel chain models later, but here we restrict ourselves to examining orientation effects in the proposed model.

In order to achieve this aim simply, a three-dimensional assemblage of randomly packed spheres is used. A short segment length of all-*trans* PE chain is positioned at the centre of each sphere, the rotation of each about its own long axis being completely random. The orientations of the segment axes are distributed within a prescribed uniaxial

orientation distribution function, f , which varies from 0 to 1 with increasing mutual alignment of the segments:

$$f = 1/2(3\langle \cos^2 \alpha \rangle - 1) \quad (11)$$

where α is the angle between the segment axis and a common director. The results are compared in Figure 11. Although this is not intended to be an exact model of PE (consider the limited connectivity and the predominance of all-*trans*) the general trends observed are applicable. It is clear that a considerable degree of orientational correlation is needed before there is a significant effect on the scattering pattern. If we consider the chain conformation, then there will be a small volume fraction of the material in which there are significantly anisotropic sequences of all-*trans* chains, despite the irregularity. The fraction of chain segments with an aspect ratio > 3 will be $\sim 6\%$. It is expected that the geometry of these segments will generate a small degree of correlation of segmental orientation, which depends upon temperature. Thus these segments may be the source of the weak orientational effects seen in n-alkanes.

TESTING ESTABLISHED MODELS

An advantage of the current approach of comparing the X-ray scattering observed with that calculated from models is that any proposed model may be easily evaluated if enough structural parameters have been specified. In this section we will examine the bundle model proposed by several authors, the Meander model of Pechhold^{17,58}, and the random coil model of Flory.

Bundle model

The bundle model has been derived to explain the intuitive feeling that random chains could not be packed sufficiently well to achieve the observed density, and has received support from some rather casual interpretations of the intense maxima in the scattering function or its associated damped oscillation in the *RDF*. The work of Ryckaert *et al.* and Vacatello *et al.* has dispelled the packing argument and we have recently shown (Mitchell, Lovell and Windle²⁴) that the existence of a prominent inter-chain maximum in the scattering is not necessarily associated with arrays of parallel chains.

Numerous studies (for example, see references 59, 60) of the packing of rigid rods, semiflexible chains and other anisotropic shapes have shown that unless the aspect ratio of the structural unit is greater than some value between 3 and 6 (the exact value varying with the method employed) substantial orientational correlation is very unlikely. We have established that the chain conformation for PE melt is irregular but, to show the scattering from as wide a range of models as possible, the bundle model is included. In order to achieve an aspect ratio of 3 a segment length of 15 \AA (12 bonds) is required. In the following bundle models chain lengths of 15 and 30 \AA will be used, and since most proposals for the bundle model have scant quantitative information, the following additional specification will be made. There will be no longitudinal register or axial rotational correlation between chains. The chains will be packed using three modes: the first is hexagonal packing, the second is a packing scheme which locally alternates square and hexagonal packing and the third uses coordinates from randomly packed discs. The

Table 2 Inter-chain distances

	Lateral packing scheme		
	Hexagonal	'Five fold'	'Random discs'
Chain spacing	5.19Å	5.00Å	4.50Å

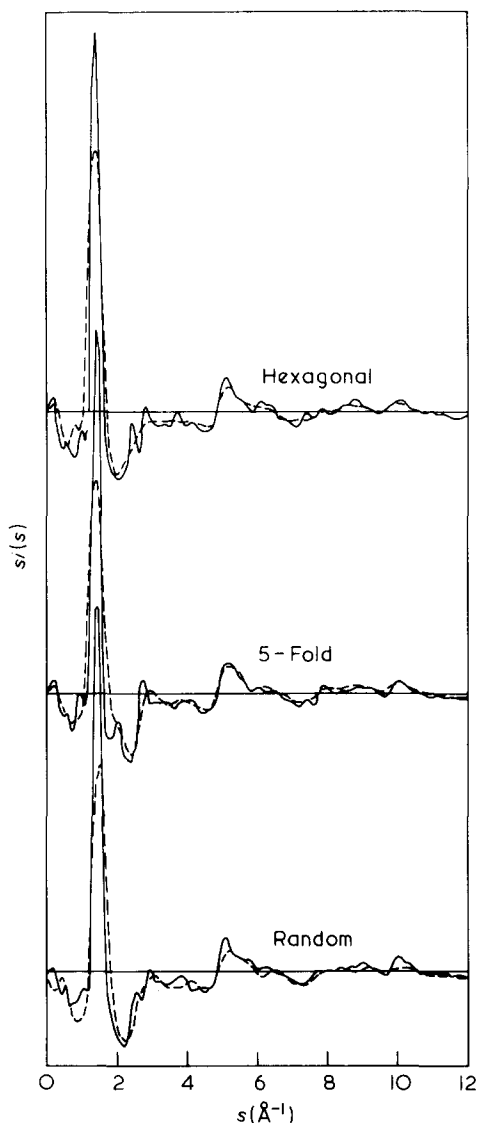


Figure 12 Scattering as $s_i(s)$ plots calculated according to the precepts of the bundle model, for different regimes of two-dimensional packing and different model sizes (— 30Å long, --- 15Å long). There is little agreement with the experimental curve (Figure 13)

latter two schemes are more fully described elsewhere⁶¹. Once the two-dimensional packing scheme is fixed and the axial repeat per chain unit is known, then the inter-chain distance may be calculated from the bulk density. If there is to be no correlation between the chains then the inter-chain distance must be similar to the diameter of a cylinder to enclose the chain, which is 5.1 Å. The scattering from the three types of model based on the inter-chain distances in Table 2 are shown in Figure 12. In addition to the differences between the experimental $s_i(s)$ curves and those calculated for scattering vectors $> 2.0 \text{ Å}^{-1}$, the main peak is at too large a scattering vector,

too narrow and too intense, and there are obvious higher order peaks at 2.0 Å^{-1} . Thus we conclude that the experimental curve does not in any respect support a bundle model for molten polyethylene. However, there is broad agreement between the calculated $s_i(s)$ curves for the bundle models, and the $s_i(s)$ curves derived from experimental data for radiation amorphized PE²⁰. Although we have not refined the bundle models to fit exactly the density of amorphized PE, we can conclude that there is considerably more inter-chain orientational correlation and a greater persistence of all-*trans* conformation, than is observed in the polyethylene melt.

Meander model

Whilst the typical conformation of chains in the meander model of Pechhold *et al.*^{17,58} is well specified, there is not sufficient information given regarding chain packing to enable models to be constructed with the desired density. As a consequence we have restricted our examination to the intra-chain component of the $s_i(s)$ curve at scattering vectors greater than $s = 2$. In the model, kinks with sequences of $gt\bar{g}$ and $\bar{g}tg$ are inserted at random into an otherwise all-*trans* PE chain. The proportion of kinks has been chosen to give 40% *gauche* bonds. The $s_i(s)$ curve for this chain (Figure 13) contains sharp features and also additional peaks not evident in the experimental curve. The sharp features indicate that the introduction of *gauche* links *via* sequences such as $gt\bar{g}$ preserves the overall chain direction and also, *per se*, preserves the long range axial repeat. More recently the meander model has been revised to include more disorder⁵⁸, and such a model may provide a better fit to the experimental data. However the less specific the conformation of the chain, the more it approaches that appropriate to a random coil model, and the more tenuous the superstructure envisaged in such an arrangement becomes. The question to be faced is how much additional disorder needs to be introduced in the meander model before the individual chains assume, in effect, a random coil trajectory.

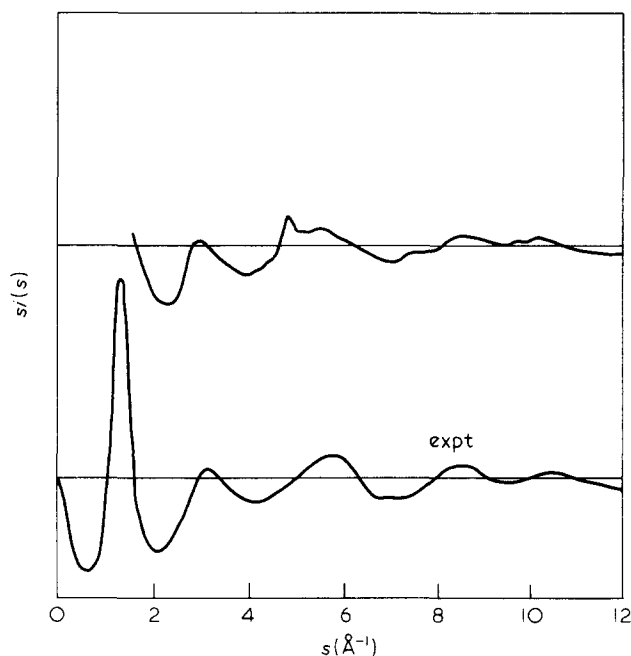


Figure 13 Calculated $s_i(s)$ curve for the Meander model with $P_t = 0.6$ compared with the experimental curve

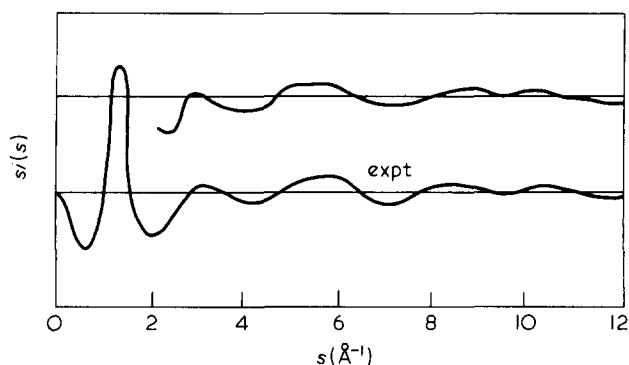


Figure 14 Scattering for a random chain built according to the statistical weights (for a temperature of 400K) proposed in the literature³². The curve is similar to that of Figure 7. $E_{g-t} = 500 \text{ cal mol}^{-1}$

Random coil

A random coil model is one in which the chains adopt a conformation applicable to an isolated chain. There is no specification of how these irregular chains pack other than it does not perturb the conformation. The scattering for a random chain built using conditional probabilities (see 'Local Conformation' section) appropriate to the statistical weights given by Abe, Jernigan and Flory³⁵ is shown in Figure 14. In essence the chain conformation and the resulting $si(s)$ curve are very similar to those in Figure 8 which are the result of a slightly more refined calculation. The agreement obtained between the experimental and calculated scattering for the random coil model must be seen as providing strong support for this model.

RADIAL DISTRIBUTION FUNCTIONS

Despite the advantages of utilizing the scattering functions for this analysis, which have been outlined already, radial distribution functions remain a useful and complementary component of any investigation. *RDF*'s highlight different aspects of the structure from those which are prominent in the $si(s)$ curves; for example, the covalently bonded distances are easily seen. To illustrate how the preceding analysis could have been made by using *RDF*'s, we have calculated *RDF*'s for two contrasting chain conformations. The first chain has an irregular conformation defined using three rotation states with 40% of the bonds in the *gauche* state. The comparable $si(s)$ curve is Figure 6. The second chain is an all-*trans* sequence, the equivalent $si(s)$ curve being Figure 4. The *RDF*'s were calculated using the techniques described by Waring, Lovell, Mitchell and Windle⁷, and Mitchell³². The *RDF*'s ($4\pi r^2(p_r - p_0)$) shown in Figure 15 clearly emphasize the distances at 1.5 Å and 2.5 Å determined by the covalent bonds. The main difference between the two calculated curves is the peak at 3.0 Å in the *RDF* for the irregular chain. This peak is absent for the all-*trans* chain, and as was first shown by Voigt-Martin and Miljhoff⁴ arises from a *trans-gauche* pair of bonds. The peak at 3.9 Å which is present in both curves is related to *trans-trans* sequences. By comparing the relative heights of this type of peak in *RDF*'s calculated from models with that obtained by experiment, results similar to those obtained from the scattering analysis may be obtained, namely an irregular chain containing about 40% *gauche* bonds. The

difficulty of using *RDF*'s arises because any peaks representing longer range intra-chain correlations are lost amongst the damped ripple corresponding to the inter-chain interactions.

CONCLUSIONS

This work has been concerned with the derivation of the structural parameters describing the local organization of PE chains in the melt phase. We have established experimentally that the conformation may be described using a three rotation state system of *trans*, *gauche* and *-gauche*, with about 60% *trans* and 40% *gauche*. This irregular conformation does not contain *gauche* pairs of opposite sign. The energy difference between *trans* and *gauche* states obtained, that is 500–700 cal mol^{-1} , compares favourably with that obtained both by spectroscopy and by theoretical considerations.

The packing of these irregular chains generates limited interactions, which are similar to those for non-anisotropic units. It is not necessary to invoke any correlation of segmental orientation in order to provide complete agreement between models and experiment. For amorphized PE, we suggest the structure is considerably more ordered, and consists of regions of parallel chains in all-*trans* conformation, with inter- and intra-molecular correlation distances of at least 25 Å.

In this work we have evaluated the extremes of models, and this reinforces the concept that in structural analysis it is not only necessary to show that one model fits but it is equally important to show that no other type of model provides satisfactory agreement. Such an approach emphasizes the value of models which are quantitatively defined rather than simple representations or sketches.

It is interesting to note that in 1953 Charlesby¹² made calculations which have a similar basis to the

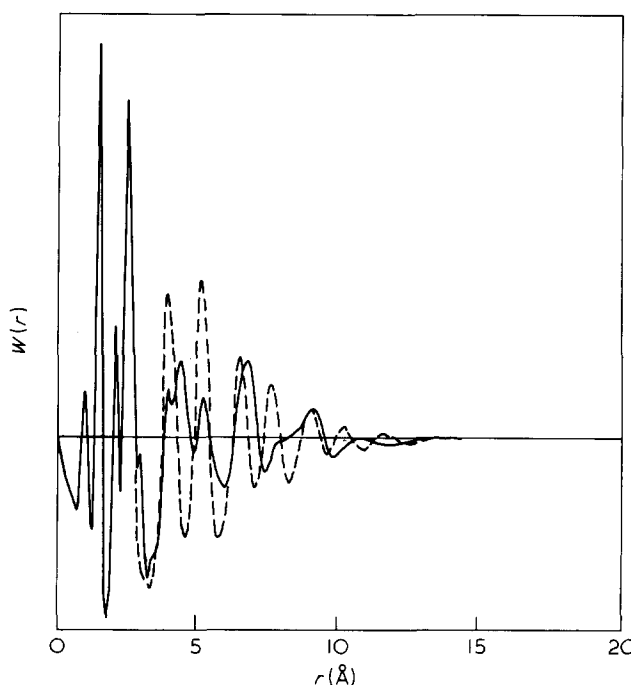


Figure 15 Comparison between *RDF*'s which are equivalent to the calculated scattering of Figure 6 (three state model, $P_t = 0.6$) continuous curve and of Figure 4 (all-*trans* chain, 10 bonds long) broken curve

conformational analysis made above, although it was confined to straight chains. We suggest that there is much to be gained by detailed and careful analysis of the scattering and the derived real space function, particularly by comparisons with models directly related to the local structure of non-crystalline polymers.

Thus on the basis of WAXS measurements alone it is possible to propose that the structure of molten polyethylene consists of random chains containing 60% *trans* bonds, and thus an energy difference of 500–700 cal mol⁻¹. There is no substantial correlation in orientation between neighbouring chains.

ACKNOWLEDGEMENTS

We thank John Finney of Birkbeck College, London, for the coordinates of the randomly packed spheres, Professor R. W. K. Honeycombe for the provision of laboratory facilities, and the Science Research Council for funding (GRB 28088).

REFERENCES

- Schelten, J., Ballard, D. G. H., Wignall, G. D., Longman, G. and Schmatz, W. *Polymer* 1976, **17**, 751
- Lieser, G., Fischer, E. W. and Ibel, K. *J. Polym. Sci., Polym. Lett. Edn.* 1975, **13**, 39
- Wignall, G. D., Ballard, D. G. H. and Schelten, J. *J. Macromol. Sci.-Phys.* 1976, **B12**, 75
- Voigt-Martin, I. and Mijlthoff, F. C. *J. Appl. Phys.* 1975, **46**, 1165; 1976, **47**, 3942
- Ovchinnikov, Yu. K., Markova, G. S. and Kargin, V. A. *Polym. Sci. USSR* 1969, **11**, 369; 1975, **17**, 2081
- Lovell, R., Mitchell, G. R. and Windle, A. H. *Faraday Discussions* 1979, **68**, 46
- Waring, J. R., Lovell, R., Mitchell, G. R. and Windle, A. H. *J. Mat. Sci.* 1982, **17**, 1171
- Fischer, E. W. and Dettenmaier, M. *J. Non-Cryst. Solids* 1978, **31**, 181
- Longman, G. W., Wignall, G. D. and Sheldon, R. P. *Polymer* 1979, **20**, 1063
- Lovell, R., Mitchell, G. R. and Windle, A. H. *Acta Cryst.* 1979, **A35**, 598
- Finbak, C. *Acta Chem. Scand.* 1949, **3**, 1279
- Stewart, G. W. *Phys. Rev.* 1928, **31**, 174
- Katz, J. R. *Trans. Faraday Soc.* 1936, **32**, 77
- Warren, B. E. *Phys. Rev.* 1933, **44**, 969
- Charlesby, A. *J. Polym. Sci.* 1953, **10**, 201
- Kan, S. and Seto, T. *Rep. Prog. Polym. Phys. Jpn.* 1976, **19**, 219
- Pechhold, W., Hauber, M. E. T. and Liska, E. *Kolloid. Z.* 1973, **251**, 818
- Petermann, J. and Gleiter, H. *Phil. Mag.* 1973, **28**, 271
- Fischer, E. W., Strobl, G. R., Dettenmaier, M., Stamm, M. and Steidle, N. *Faraday Discussions* 1979, **68**, 26
- Yoda, O., Kuriyama, I. and Odajima, A. *J. Appl. Phys.* 1978, **49**, 5468
- Gupta, M. and Yeh, G. S. Y. *J. Macromol. Sci.-Phys.* 1979, **16**, 225
- Boyer, R. F. *J. Macromol. Sci.-Phys.* 1975, **B12**, 253
- Ovchinnikov, Y., Antipov, E. M., Markova, G. and Bakeev, N. *Makromol. Chem.* 1976, **177**, 1567
- Mitchell, G. R., Lovell, R. and Windle, A. H. *Polymer* 1980, **21**, 989
- Brady, G. W. and Fein, D. B. *J. Appl. Cryst.* 1975, **8**, 261
- Colebrooke, A. and Windle, A. H. *J. Macromol. Sci.-Phys.* 1976, **B12**, 373
- Lovell, R. and Windle, A. H. *Polymer* 1981, **22**, 175
- Mitchell, G. R. and Lovell, R. *Acta Cryst.* 1981, **A37**, 189
- Lovell, R. and Windle, A. H. *Polymer* 1976, **17**, 488
- Warren, B. E., 'X-Ray Diffraction', 1969, Addison Wesley, p. 117
- International Tables for X-Ray Crystallography (1974) Vol. IV, Birmingham, Kynoch Press
- Mitchell, G. R. *Acta Cryst.* 1981, **A37**, 487
- Guinier, A. and Fournet, G. 'Small Angle Scattering of X-Rays', 1955, New York, Wiley
- Scott, R. A. and Scheraga, H. A. *J. Chem. Phys.* 1966, **44**, 3054
- Abe, A., Jernigan, R. L. and Flory, P. J. *J. Am. Chem. Soc.* 1966, **88**, 631
- Lal, M. and Spencer, D. *Mol. Phys.* 1971, **22**, 649
- D'Ilario, L. and Giglio, E. *Acta Cryst.* 1974, **B30**, 372
- McMahon, P. E. *Trans. Faraday Soc.* 1965, **61**, 7
- Boyd, R. H. and Breitling, S. M. *Macromolecules* 1972, **4**, 1
- Hopfinger, A. J. 'Conformational Properties of Macromolecules', 1973, Academic Press, New York
- Momany, F. A., Carruthers, L. M., McGuire, R. F. and Scheraga, H. A. *J. Phys. Chem.* 1974, **78**, 1595
- Atkins, E. D. T., Isaac, D. H. and Keller, A. *J. Polym. Sci. Polym. Phys. Edn.* 1980, **18**, 71
- Brant, D. A., Miller, W. G. and Flory, P. J. *J. Mol. Biol.* 1967, **263**, 47
- Scheraga, H. A. 'Advances in Physical Organic Chemistry', (Ed. V. Gold), 1968, Academic Press, London, p. 103
- Volkenstein, M. W. 'Configurational Statistics of Polymeric Chains', 1959, Interscience, New York
- Flory, P. J. 'Statistical Mechanics of Chain Molecules', 1969, Interscience, New York
- Scherer, J. R. and Snyder, R. G. *J. Chem. Phys.* 1980, **72**, 5798
- Slomimskii, G. L., Askadskii, A. A. and Kitaigorodskii, A. I. *Polym. Sci. USSR* 1970, **12**, 556
- Stewart, C. W. and von Frankenberg, C. A. *J. Polym. Sci. A-2* 1967, **5**, 623
- Finney, J. L. p. 35, 'The Structure of Non-Crystalline Materials', (Ed. P. H. Gaskell), 1977, Taylor and Francis, London
- Theile, E. *J. Chem. Phys.* 1963, **39**, 474
- Wright, A. C. *Disc. Faraday Soc.* 1970, **50**, 111
- Blum, L. and Stell, G. *J. Chem. Phys.* 1979, **71**, 42; 1980, **72**, 2212
- de Vrij, A. *J. Chem. Phys.* 1979, **71**, 3267
- Ryckaert, J. and Bellemans, A. *Faraday Discussions* 1978, **66**, 95
- Vacatello, M., Avitabile, G., Corradini, P. and Tuzi, A. *J. Chem. Phys.* 1980, **73**, 548
- Weber, T. A. and Helfand, E. *J. Chem. Phys.* 1979, **71**, 4760
- Pechhold, W. R. and Grossman, H. P. *Faraday Discussions* 1979, **68**, 58
- Flory, P. J. *Proc. Roy. Soc. (London)* 1956, **A234**, 60
- Cotter, M. A. 'The Molecular Physics of Liquid Crystals', (Eds. G. R. Luckhurst and G. W. Gray), 1979, Academic Press, London, p. 169
- Mitchell, G. R. unpublished *Thesis (CNA A)* 1982